World Academy of Science, Engineering and Technology
International Journal of Electrical and Computer Engineering
Vol:3, No:10, 2009

Optimum Control Strategy of Three-Phase Shunt Active Filter System

Mihaela Popescu, Alexandru Bitoleanu, Mircea Dobriceanu, and Vlad Suru

***Abstract*—**The aim of this paper is to identify an optimum control strategy of three-phase shunt active filters to minimize the total harmonic distortion factor of the supply current. A classical PI-PI cascade control solution of the output current of the active filter and the voltage across the DC capacitor based on Modulus–Optimum criterion is taken into consideration. The control system operation has been simulated using Matlab-Simulink environment and the results agree with the theoretical expectation. It is shown that there is an optimum value of the DC-bus voltage which minimizes the supply current harmonic distortion factor. It corresponds to the equality of the apparent power at the output of the active filter and the apparent power across the capacitor. Finally, predicted results are verified experimentally on a MaxSine active power filter.

***Keywords*—**Active filtering, Controller tuning, Modulus Optimum criterion, Optimum control.

I. Introduction

IN recent years, shunt active power filters (SAPF) based on a voltage source inverter structure have been widely studied and developed as a solution to harmonic current pollution problems. They improve the power quality by injecting compensating currents into the power system based on calculated reference currents. Different complex approaches have been investigated to improve the performance tracking [1], [2]. However, to facilitate low-cost analogue control, cascade control of shunt active filter via simple and robust PI controllers is a viable solution [3].

The active power filters performance depends on the modulation technique of the static converter. Among the various pulse width modulation (PWM) techniques, the sinusoidal one seems to be frequently used because of its simplicity of implementation. Besides, in the context of closed loop control, the performances of the SAPF with sinusoidal modulation in terms of total harmonic distortion in source current and DC-bus utilization are close to space vector modulation technique performances [4]. As the modulus optimum method for optimization of regulators is applied with good performances in a wide variety of cases in the control field [5], [6], [7], the PI controller parameters can be tuned according to absolute value optimum criterion. The gain and phase margin approach is also available for high performance and robustness requirement [8].

Mihaela Popescu is with Faculty of Electromechanical, Environmental and Industrial Informatics Engineering, University of Craiova, 200440 Craiova Romania (phone: +40 251 435 255; fax: +40 251 435 255; e-mail: mpopescu@em.ucv.ro).

A. Bitoleanu is with Faculty of Electromechanical, Environmental and Industrial Informatics Engineering, University of Craiova, 200440 Craiova Romania (phone: +40 251 435 255; fax: +40 251 435 255; e-mail: abitoleanu@em.ucv.ro)..

M. Dobriceanu is with Faculty of Electromechanical, Environmental and Industrial Informatics Engineering, University of Craiova, 200440 Craiova Romania (phone: +40 251 435 255; fax: +40 251 435 255; e-mail: mdobriceanu@em.ucv.ro).

V. Suru is with Faculty of Electromechanical, Environmental and Industrial Informatics Engineering, University of Craiova, 200440 Craiova Romania (phone: +40 251 435 255; fax: +40 251 435 255; e-mail: vsuru@em.ucv.ro).

This work was supported by Romanian Ministry of Education and Research, Grant 21-010/2007.

II. Structure of the Control System

In this study, the cascade control is composed of two control loops with the voltage loop outside the inner current loop (Fig. 1). The two essential parameters to be controlled are the inverter output current and the DC-bus voltage at the inverter input from the viewpoint of active power balance. Therefore, two PI controllers are to be designed a current one and a voltage one.

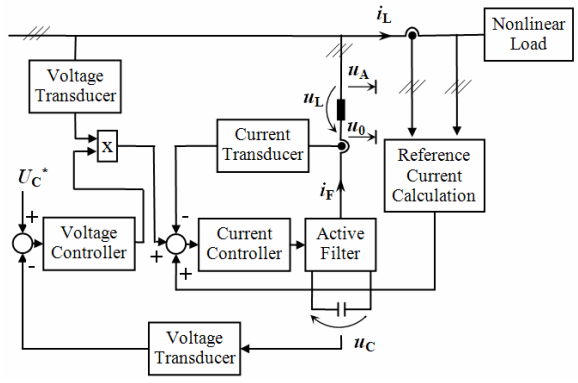

Fig. 1 Single-line block diagram of the automatic control system

In the associated block diagram of Fig. 2, the following transfer functions are pointed out: G_{Cu} – transfer function of the voltage controller; G_{Ci} - transfer function of the current controller; G_{Fi} – first partial transfer function of the active filter, from the modulating voltage signal to the output current; G_{Fu} - second partial transfer function of the active filter, from the output current to the DC-bus voltage; G_{Ti} - transfer function of the current transducer; G_{Tu} - transfer

function of the voltage transducer.

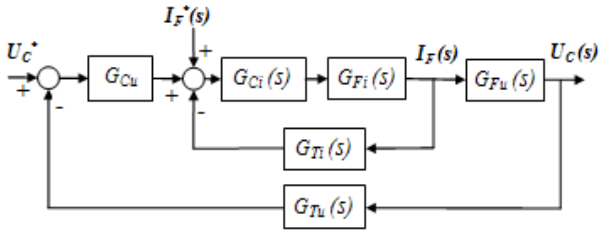

Fig. 2 Block diagram of closed-loop active filter

III. Active Power Filter Transfer Functions

As it was previously specified, the active filter intervenes in the block diagram of Fig. 2 by two transfer function [9].

A. First partial transfer function of the active power filter

Supposing that the filter output voltage (u_0) is constant and equal with its average value (U_{0av}) during a period of the carrier signal, then u_0 can be expressed as a function of the reference voltage um in the Laplace domain, i.e.

$$U_0(s)=U_{0av}(s)=\frac{U_c}{2U_{t\,max}}\cdot U_m(s), \tag{1}$$

where U_c and U_{tmax} denote the DC-bus voltage and the amplitude of triangular carrier signal.

Then, considering that the time origin corresponds to the moment when the A phase-voltage, $u_A = U_A \sin(\omega_1 t)$, passes through zero becoming positive, the Kirchhoff's voltage law at the filter output in the Laplace domain allows to express the first partial transfer function of the active filter,

$$G_{Fi}(s)=\frac{I_F(s)}{U_m(s)}=\frac{U_c}{2L\cdot U_{t\,max}\cdot s}=\frac{1}{K_{Fi}\cdot s}, \tag{2}$$

where

$$K_{Fi}=\frac{2L\cdot U_{t\,max}}{U_c}. \tag{3}$$

B. Second partial transfer function of the active power filter

Let us consider a small variation Δu_c of the voltage across the capacitor around its average value U_{cm}. Hence, the power corresponding to the energy stored in capacitor has to correspond to the whole power in the connecting point of the filter to the power supply, that is to the apparent power. Thus, the Laplace transform of the above condition allows expressing the desired transfer function,

$$G_{Fu}(s)=\frac{U_c(s)}{I_F(s)}=\frac{3U_A}{\sqrt{2}C\cdot U_{cm}\cdot s}=\frac{1}{K_{Fu}\cdot s}, \tag{4}$$

where

$$K_{Fu}=\frac{\sqrt{2}C\cdot U_{cm}}{3U_A}. \tag{5}$$

IV. Current Controller Tuning

In the block diagram of the current loop (Fig. 3), it is assumed that the dynamic behavior of the transducer-current filter can be approximated by a first-order transfer function:

$$G_{Ti}(s)=\frac{K_{Ti}}{1+T_{Ti}\cdot s}. \tag{6}$$

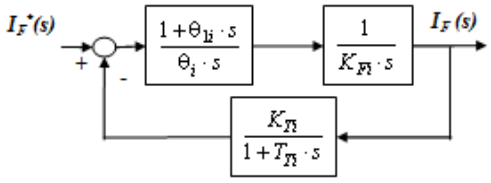

Fig. 3 Block diagram of the current loop

A classical proportional-integral structure is adopted for the current controller, i.e.

$$G_{Ci}(s)=\frac{1+\theta_{1i}\cdot s}{\theta_i\cdot s}; \tag{7}$$

To use the modulus optimum tuning criteria, the open-loop transfer function is written in the following form:

$$G_{di}(s)=G_{Ci}(s)\cdot G_{Fi}(s)\cdot G_{Ti}(s)=\frac{1+\theta_{1i}\cdot s}{T^2\cdot s^2\cdot(1+T_{Ti}\cdot s)} \tag{8}$$

where

$$T^2=\frac{\theta_i\cdot K_{Fi}}{K_{Ti}}; \tag{9}$$

As regards the transfer function of the closed-loop unity feedback system, it can be written as:

$$G_i(s)=\frac{1+\theta_{1i}\cdot s}{T^2\cdot T_{Ti}\cdot s^3+T^2\cdot s^2+\theta_{1i}\cdot s+1}. \tag{10}$$

After expressing the square of the above transfer function modulus, the simple condition of canceling the denominator coefficients which contain differences leads to the following relations:

$$\theta_{1i}=\sqrt{2}T;\qquad T=2\sqrt{2}T_{Ti}. \tag{11}$$

Taking into account (9) and (11), the two parameters of current controller are expressed:

$$\theta_{1i}=4T_{Ti};\qquad \theta_i=8K_{Ti}\cdot T_{Ti}^2/K_{Fi}. \tag{12}$$

Thus, the transfer function of the current controller is given by:

$$G_{Ci}(s)=\frac{K_{Fi}}{2K_{Ti}\cdot T_{Ti}}\left(1+\frac{1}{4T_{Ti}\cdot s}\right), \quad (13)$$

Accordingly, the open-loop and close-loop unity feedback transfer functions given by (8) and (10) become:

$$G_{di}(s)=\frac{1+4T_{Ti}\cdot s}{8T_{Ti}^2\cdot s^2\cdot(1+T_{Ti}\cdot s)}, \quad (14)$$

$$G_i(s)=\frac{1+4T_{Ti}\cdot s}{1+4T_{Ti}\cdot s+8T_{Ti}^2\cdot s^2+8T_{Ti}^3\cdot s^3}. \quad (15)$$

As the terms containing T_{Ti}^2 and T_{Ti}^3 are very insignificant compared with 1, the transfer function (15) becomes:

$$G_i(s)\approx 1. \quad (16)$$

V. Voltage Controller Tuning

A PI controller is also adopted to control the voltage across the capacitor. In the forward path of the block diagram (Fig.4), due to passing to unity feedback, there is the inverse of the current transducer transfer function. The forward transfer function can be expressed as follows:

$$G_{du}(s)=\frac{(1+\theta_{1u}\cdot s)\cdot(1+T_{Ti}\cdot s)\cdot K_{Tu}}{K_{Ti}\cdot K_{Fu}\cdot\theta_u\cdot s^2\cdot(1+T_{Tu}\cdot s)} \quad (17)$$

where θ_{1u} and θ_u are the parameters to be determined.

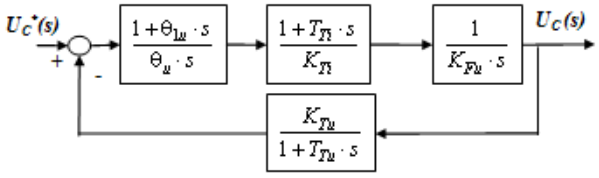

Fig. 4 Block diagram of the DC-bus voltage loop

If the time constants of the current and voltage transducers are supposed to be equals, (17) becomes:

$$G_{du}(s)=\frac{1+\theta_{1u}\cdot s}{T_u^2\cdot s^2};\qquad T_u^2=\frac{K_{Ti}\cdot K_{Fu}\cdot\theta_u}{K_{Tu}} \quad (18)$$

Then, the closed-loop unity feedback transfer function is given by:

$$G_u(s)=\frac{1+\theta_{1u}\cdot s}{1+\theta_{1u}\cdot s+T_u^2\cdot s^2} \quad (19)$$

and the square of its modulus can be expressed as:

$$M_u^2(\omega)=\frac{1+{\theta_{1u}}^2\cdot\omega^2}{1+\omega^2\cdot\left({\theta_{1u}}^2-2T_u^2\right)+\omega^4\cdot T_u^4}. \quad (20)$$

Canceling the denominator term which contains a difference in (20) gives the condition:

$$\theta_u=\frac{K_{Tu}}{2K_{Ti}\cdot K_{Fu}}\theta_{1u}^2. \quad (21)$$

It must be noticed that the above condition imposes the loop phase-margin. Thus, the open-loop transfer function, in the frequency domain, can be arranged as

$$G_{du}(j\omega)=-\frac{1+j\omega\cdot\theta_{1u}}{\omega^2\cdot T_u^2}=-\frac{1+j(\omega/\omega_1)}{(\omega/\omega_{01})^2}. \quad (22)$$

where

$$\omega_1=1/\theta_{1u};\ \omega_0=1/T_u. \quad (23)$$

Moreover, by introducing the cut-off pulsation ω_c, the associated phase margin φ_m is given by:

$$\varphi_m=arctg\left(\frac{\omega_c}{\omega_1}\right)\approx 65.5^0. \quad (24)$$

In order to find the second relation required in the voltage controller design, the passband of the unity feedback system is imposed. So, the square modulus of the closed-loop unity feedback transfer function given by (20) can be written as:

$$M_u^2(\omega)=4\cdot\frac{1+(\omega/\omega_1)^2}{4+(\omega/\omega_1)^4}. \quad (25)$$

But, as the magnitude response remains within $\sqrt{2}$ of its maximum value inside the passband, the passband frequency is obtained:

$$f_p=\frac{\omega_1}{\pi}\sqrt{\frac{1}{2}\left(\sqrt{5}-1+\sqrt{4-\sqrt{5}}\right)}. \quad (26)$$

Therefore, the time constants in the voltage controller transfer function can be expressed as follows:

$$\theta_{1u}\approx 0.36/f_p;\quad \theta_u\approx 64.95\cdot 10^{-2}\cdot\frac{K_{Tu}}{K_{Ti}\cdot K_{Fu}}\cdot\frac{1}{f_p^2}. \quad (27)$$

VI. Control System Performances

To test the performances of the control system, the block

diagram in the Fig. 2 has been implemented under Matlab-Simulink environment. The simulation parameters are: $U_A = \sqrt{2} \cdot 220$ V, $U_{cm} = 700$ V, L = 14 mH, $U_{t\,max} = 10$ V, K_{Ti} = 0.2, K_{Tu} = 0.0125, T_{Ti} = T_{Tu} = 10^{-5} s. In addition, the determined parameters in the control loops for f_p = 20Hz are: $\theta_{1u} = 0.018$ s, $\theta_u = 0.003$ s, $\theta_{1i} = 4 \cdot 10^{-5}$ s, $\theta_i = 3.73 \cdot 10^{-6}$ s, $K_{Fi} = 4.28 \cdot 10^{-5}$ s, $K_{Fu} = 3.3 \cdot 10^{-3}$ s.

In order to charge the DC-bus capacitance, a ramp voltage of 700 V is applied and then, after 0.3 seconds, the current to be compensated is applied too.

The current to be compensated is provided by a uncontrolled rectifier according to so-called p-q theory [10], [11]. The response of the current loop compared with the reference current (Fig. 5) illustrates a low average square error of 1.06 A which confirms the very good behavior of the control system. After an overshoot of 5.8%, the DC-bus voltage practically keeps its reference value (Fig. 6).

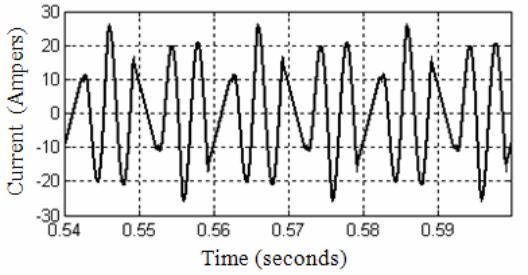

Fig. 5 Current loop response in case of non controlled rectifier load

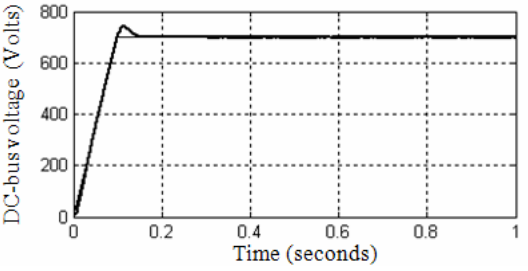

Fig.6 DC-bus voltage response in case of non controlled rectifier load

VII. DC-Bus Voltage Influence and Connection with Reactive and Distortion Compensating Powers

Analytic analysis of the phenomena associated of an active power filter operation is very difficult especially owing to the PWM control of the voltage inverter.

The use of some simplifying assumptions could misrepresent the reality and consequently lead to conclusions very far off from the physical phenomenon. For this reason, we have chosen the Matlab-Simulink environment facilities to model and simulate the shunt active filter.

The nonlinear load taken into consideration is an uncontrolled rectifier supplying a load of RLC type.

At constant load, the operation of the active filter for different DC-bus set-point voltages has been analyzed based on the calculation of the powers occurring in the system and on the total harmonic distortion factor (*THD*) of the supply current.

The p-q theory of the power has been used to express the apparent power S_f, active power P, reactive power Q and distortion power D_f [12]:

$$S_f = \sqrt{\frac{1}{2\pi}\int_0^{2\pi} |\underline{s}|^2 d(\omega t)}\,; \tag{28}$$

$$P = \frac{1}{T}\int_{t-T}^{t} p\,dt\,; \tag{29}$$

$$Q = \frac{1}{T}\int_{t-T}^{t} q\,dt\,; \tag{30}$$

$$D_f = \sqrt{\frac{1}{2\pi}\int_0^{2\pi}\left(p_{\sim}^2 + q_{\sim}^2\right)d(\omega t)} = \sqrt{S_f^2 - P^2 - Q^2}\,, \tag{31}$$

where $\underline{s}$ is the complex apparent power, p and q are its real and imaginary parts and $p_{\sim}$ and $q_{\sim}$ are the AC components of p and q.

The following expressions have been used to calculate the active (P_c) and reactive (S_c) powers across the DC capacitor:

$$P_c = U_c I_{cav} = U_c\left(\frac{1}{T}\int_{t-T}^{T} i_c\,dt\right), \tag{32}$$

$$S_c = U_c I_{crms} = U_c\sqrt{\frac{1}{T}\int_{t-T}^{T} i_c^2\,dt}\,, \tag{33}$$

The simulation results have been processed and represented in a graphic form.

Thus, the dependence in Fig. 7 reveals an optimum value of the DC-bus voltage which minimizes the supply current *THD*.

As it can be seen in Fig. 7, keeping the DC-bus voltage at its optimum value (i.e. of about 660V for the analyzed case study) leads to a diminution of the current *THD* from 30.5% to 5.6%. The same aspect is made evident by the current waveforms in Fig. 8.

The current provided by the compensating capacitor contains the harmonics to be compensated and points out the switching frequency of the voltage inverter (Fig. 9).

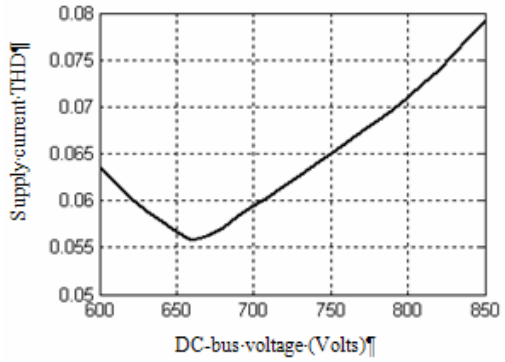

Fig. 7 Supply current *THD* versus DC-bus voltage for a load current *THD* of 0.305

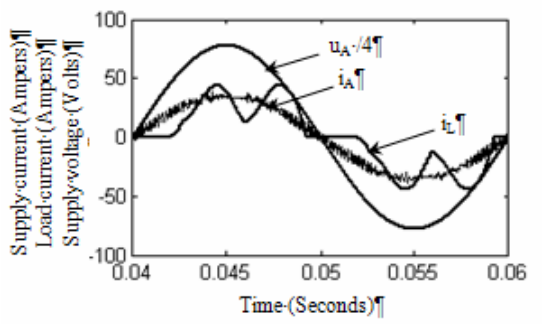

Fig. 8 Waveforms of supply voltage (u_A), supply current (i_A) and load current (i_L) for DC-bus voltage of 660V and load current *THD* of 0.305

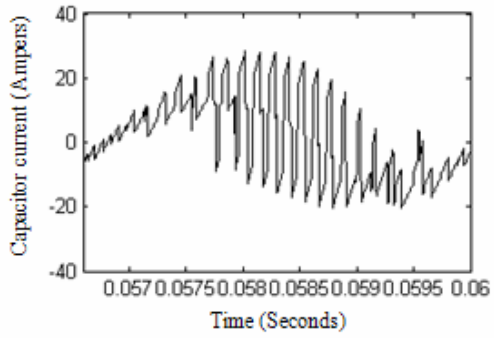

Fig. 9 Capacitor current waveform for DC-bus voltage of 660V and load current *THD* of 0.305

Interesting information is given by the dependence of the powers in the system on the voltage across the capacitor (Fig.10).

It can be seen that the powers at the AC side of the active filter are a little influenced by the DC-bus voltage value. Actually, the active power has a little diminution and the distortion power has a little increase as the DC-bus voltage increases. This aspect illustrates the correctness of the hypothesis made for obtaining the transfer function $G_{Fu}(s)$ given by expression (4) and can be used in implementation an optimum control system.

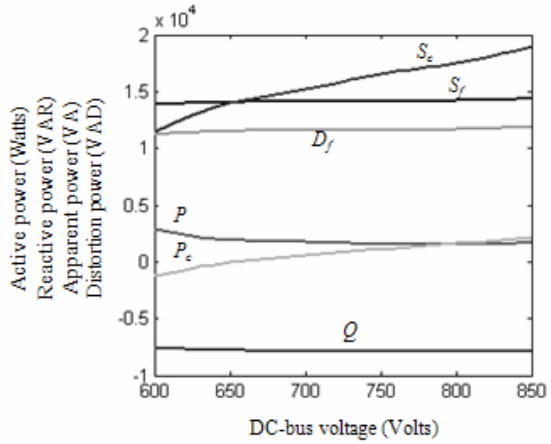

Fig. 10 Powers versus DC-bus voltage

The detailed analysis shows that the optimum value of the DC-bus voltage linearly depends on the power to be compensated. Actually, this is the second possibility of implementing an optimal control system.

VIII. Experimental Results

The simulation results have been verified by experimental way through a MaxSine active power filter manufactured by Nokian Capacitors Ltd. The harmonic spectrum (up to 500th order) of the filtered current for the optimum value of DC voltage (i.e. 660V) is shown in Fig. 11.

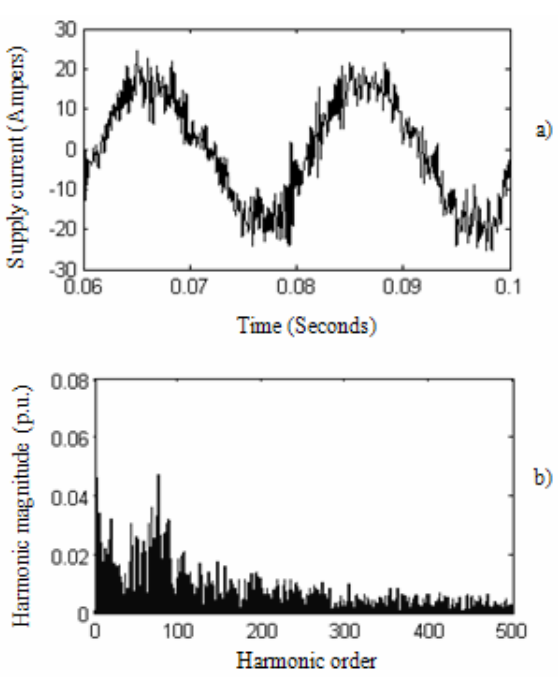

Fig. 11 Supply current waveform (a) and its harmonic spectrum (b) for optimum DC-bus voltage value

The next figure shows the harmonic spectrum of the current in the case of a DC-bus voltage of 750V. As it can be seen in Fig. 11 and Fig. 12, the current waveform is much improved at the optimal value. Quantitatively, the current *THD*

diminishes two times, from 41% to 21%. It must be noticed that the partial harmonic distortion factor calculated by taking into consideration only the first 51 harmonics is of about 8% and it has an insignificant modification. This aspect is explained by the fact that the DC-bus voltage value has a significant influence on the high order harmonics generated by the PWM frequency.

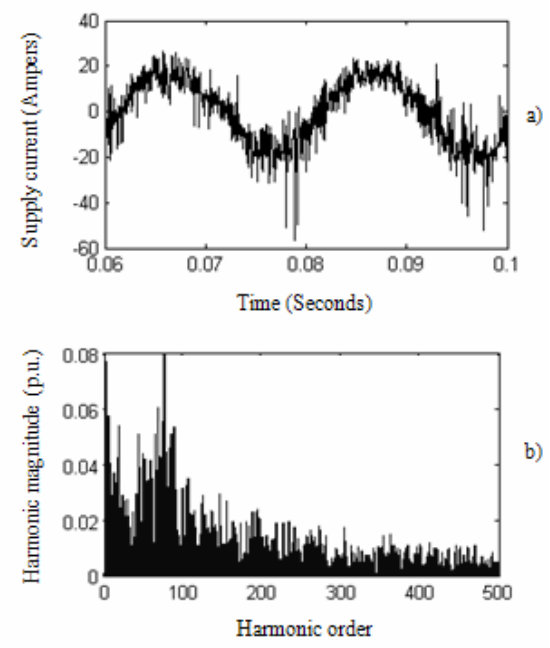

Fig. 12 Supply current waveform (a) and its harmonic spectrum (b) for a DC-bus voltage value of 750V

IX. Conclusions

The control system of the active power filter is composed of an inner current loop and an outer voltage loop, both of them based on conventional PI controllers. The whole controllers tuning is done according modulus optimum criterion.

It is shown that the modulus optimum criterion gives a relationship between the PI voltage controller parameters which imposes a good loop phase-margin. In addition, to tune the DC-bus voltage controller, the passband of the unity feedback system is imposed.

The simulations performed using the Matlab-Simulink environment illustrate a very good behavior of the control system regarding reference tracking.

At constant load, it is shown that there is an optimum value of the DC-bus voltage which minimizes the supply current *THD*. It corresponds to the equality of the apparent power at the output of the active filter and the apparent power across the capacitor.

The close agreement between the simulation and the experimental results proves the validity of the analysis.

References

[1] C.T. Pan, Y.S. Huang, and T.L. Jong, "A Constantly sampled current controller with switch status dependent inner bound," *IEEE Trans. Ind. Electronics*, vol. 50, no. 3, pp. 528-534, June 2003.

[2] B. Mazari and F. Mekri, "Fuzzy hysteresis control and parameter optimization of a shunt active power filter," *Journal of Information Science and Engineering*, 21, pp. 1139-1156, 2005.

[3] K.M. Tsang and W.L. Chan, "Design of single-phase active power filter using analogue cascade controller," *IEE Proc.-Electr. Power Appl., vol. 153*, no. 5, pp.735-741, September 2006.

[4] J. Chelladurai, G. Saravana Ilango, C. Nagamani, and S. Senthil Kumar, "Investigation of various PWM techniques for shunt active filter," *International Journal of Electrical Systems Science and Engineering*, vol. 1 no. 2, pp.87-93, 2008.

[5] K.J. Astrom and T. Hagglund, "PID controllers theory: Design and tuning," Instrument Society of America, Research Triangle Park, 1995.

[6] A.J.J. Rezek, C.A.D. Coelho, J.M.E. Vicente, J.A. Cortez, and P.R. Laurentino, "The modulus optimum (MO) method applied to voltage regulation systems: modeling, tuning and implementation," in *Proc. International Conf. on Power System Transients*, 24-28 June 2001, Rio de Janeiro (Brazil).

[7] C. Bajracharya, M. Molinas, J.A. Suul, and T. M.Undeland, "Understanding of tuning techniques of converter controllers for VSC-HVDC," in *Proc. Of Nordic Workshop on Power and Industrial Electronics*, Espoo (Finland), June 9-11, 2008.

[8] C.H. Lee, "A survey of PID controller design based on gain and phase margins," *International Journal of Computational Cognition*, vol. 2, no..3, pp. 63–100, September 2004.

[9] P. Ladoux and M. Metz, "Utilisation de l'onduleur de tension mli pour la correction du facteur de puissance," *La revue 3E.I*, no. 28, pp. 5-15, March 2002.

[10] E.H. Watanabe, R.M. Stephan, and M. Aredes, "New concept of instantaneous active and reactive powers in electrical systems with generic loads," *IEEE Transactions on Power Delivery*, vol. 8, pp. 697-703, 1993.

[11] A. Bitoleanu, M. Popescu, M. Dobriceanu, and F. Nastasoiu, "Current decomposition methods based on p-q and CPC theories for active filtering reasons," *WSEAS Transactions on Circuits & Systems*, vol. 7, pp. 869-878, October 2008.

[12] A. Bitoleanu, M. Popescu, M. Dobriceanu, "A New Interpretation of the Phasor Theory on Powers under Non-Sinusoidal Current," ACEMP'07 and ELECTROMOTION'07 Joint meeting, Bodrum Turkey, 10-12 September 2007.